

---

# GRADED DAMAGE SOLUTIONS IN ONE DIMENSION

---

A PREPRINT

✉ **Nunziante Valoroso**

Dipartimento di Ingegneria  
Università di Napoli Parthenope  
Napoli, 80143  
nunziante.valoroso@uniparthenope.it

April 21, 2023

## ABSTRACT

A regularized damage model is considered named *Graded damage* in which the gradient enhancement has the form of an explicit bound for the spatial gradient of damage. The key features of the proposed approach are demonstrated by computing the analytical solution of two problems that are one-parameter dependent. The first one is the classical one-dimensional damageable rod under tensile load, for which the hardening function is determined based on the equivalence with a given cohesive relationship. The second application is a mode-I delamination problem for which the cohesive law for the interface is formulated starting from the graded damage concept, i.e. by prescribing the shape of damage distribution within the cohesive process zone.

**Keywords** Damage mechanics · Regularization · Cohesive zone models

## 1 Introduction

Damage and Fracture Mechanics find their *raison d'être* in the need for predictive computations able to prevent catastrophic failure in engineering structures. The complexity of the physics of damage, which rules out any homogeneity of materials at the usual macroscopic scale of laboratory experiments, has led to many different modeling assumptions in Solid Mechanics, each of them resulting from a suitable trade-off between physical relevance at different scales and applicability to structural design Bažant and Planas (1998). Nonetheless, computations of failure mechanisms and ultimate load-carrying capacity of structures still stay as difficult tasks in civil and mechanical engineering owing to the intrinsic non-smoothness of damage and fracture phenomena François et al. (2013).

Roughly speaking, one can categorize the computational approaches to failure into two families, the continuous and the discontinuous one, each of them with advantages and limitations. Discontinuous descriptions allow for jumps in the displacement field, whereby one has to deal with changes in topology that are intrinsic to the representation of discrete cracks. In a finite element context this requires special elements with embedded discontinuities Armero and Garikipati (1996) or extended finite element formulations (X-FEM) either in the original setup of Belytschko and co-workers Moës et al. (1999) or in the format of the so-called *Thick Level Set* model Moës et al. (2011).

One can also include into the discontinuous family the cohesive zone models originating from the work of Barenblatt Barenblatt (1962). Initially motivated by the need to characterize stress states in the vicinity of cracks, in cohesive zone models one may speak e.g. of damage, delamination or de-cohesion to designate all those progressive phenomena preceding fracture, during which material separation is resisted by attractive forces that develop along an extended crack tip, i.e. the *cohesive process zone*.

In the cohesive zone approach crack progression is governed by an independent relationship between surface tractions and displacement jumps that incorporates typical fracture parameters, i.e. the cohesive strength and the fracture toughness. Under certain conditions the shape of the softening curve does also play a role in fracture predictions Alfano (2006), but it is commonly believed to be less relevant compared to the other parameters. Anyway, classical implementations of the cohesive zone concept only allow for strong discontinuities along interfaces that pre-exist in the material

before any loading, whereby in numerics use is made of degenerated (zero-thickness) finite elements that are placed along potential discontinuity surfaces Mi et al. (1998).

A discrete crack representation closely reflects the physics of fracture but includes a number of difficulties, most of which are related to crack tracking. This partly motivates the continuous approach as a tool for modeling fracture starting from the strain localization stage; here no physical crack opening exist and fully damaged states can be understood as the smeared, diffuse representation of macro-fractures. In this context the basic idea consists of preserving the topology of the initial finite element mesh and to bring into the material model a concise information about material microstructure via a length scale parameter; the latter is used to introduce the necessary regularization that restores well-posedness of the problem either via a nonlocal integral approach after Pijaudier-Cabot and Bažant Pijaudier-Cabot and Bažant (1987) or in the form of a gradient enhancement in the wake of the works of Peerlings et al. Geers et al. (1998); Peerlings et al. (1996). We also note the family of *phase-field models* initiated from the regularized form of the variational theory of quasi-static fracture Bourdin et al. (2000); though starting from a different perspective, i.e. global energy minimization, these models end up with a field equation of diffusive type that is quite close to that of gradient damage models, see e.g. Miehe et al. (2010a,b) among others.

In all such cases averaging or differential operators come into play, whereby the constitutive equations are no longer defined at the local level but are established at the scale of the structural model. One may then conclude that continuous representations of discontinuities provide globally smoothed solutions through elements, whereas in usual local models stresses, strains and internal variables are all defined in a point-wise fashion that can be understood as generally discontinuous fields inside elements and across elements boundaries Alfano et al. (1998).

This chapter is concerned with a gradient-based continuum damage formulation named *Graded damage* Valoroso and Stolz (2022), i.e. a Generalized Standard Model with convex constraints that admits the geometrical interpretation of the Thick Level Set approach of Moës et al. Moës et al. (2011). The variational structure of the model along with its directional convexity properties allow for an effective implementation based on convex programming in the spirit of *direct methods*, by alternating minimization with respect to displacements and damage and maximization with respect to the Lagrange multipliers that implicitly contain the information necessary to track the interphases between fully damaged regions and the sound material.

In particular, in the following the graded damage model is applied to two different one-dimensional problems for which a non-homogeneous solution is computed in closed form. The first problem is presented in Section 2; it is rather classical and refers to the rod under tensile load, whose interest lies in the fact that the relevant solution is considered to be representative of the response of a three-dimensional structure across a localization band. Moreover, this analytical solution is typically used to design the constitutive functions of a continuum damage formulation that render the response of the damageable rod identical to the one of an elastic bar in which a cohesive interface is the only source of dissipation, see e.g. Lorentz and Godard (2011); Wu (2017).

The second problem is discussed in Section 3; it is in a sense analogous to the one of the tensile rod and refers to a one-parameter-dependent delamination problem where the interface constitutive relationship is gradient-enhanced based on the graded damage concept. Worth noting is the fact that in cohesive models understood in the sense of Hillerborg Hillerborg et al. (1976) there is in principle no need for any regularization, whereby few attempts have been made so far to introduce gradients along a cohesive interface. However, the general consensus that nonlocal interactions may occur at the meso-scale level suggest that introduction of a material length scale into an interface model is a worthwhile attempt Latifi et al. (2017); Nguyen et al. (2016).

## 2 The damageable rod

To begin with, consider the homogeneous elastic-damageable rod depicted in Figure 1; the domain  $\Omega$  occupied by the structure is the interval  $[-L, L]$ , body forces are neglected and loading is performed via an increasing elongation at the two ends of the bar.

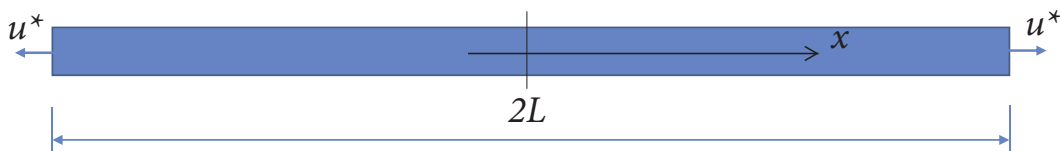


Figure 1: One-dimensional rod. Model problem.

In the present one-dimensional context the stored energy function reads:

$$\psi(u, d) = \frac{1}{2} \omega(d) E \left( \frac{du}{dx} \right)^2 \quad (1)$$

where  $E > 0$  is the elastic modulus,  $u$  is the axial displacement obeying the essential boundary conditions:

$$u(-L) = -u^*, \quad u(L) = u^*; \quad u^* > 0 \quad (2)$$

$d$  is the damage variable and  $\omega(d)$  is a monotonically decreasing function that accounts for material degradation.

Restricting attention to the class of Generalized Standard Materials, the local model is completed by prescribing a dissipation pseudo-potential Halphen and Nguyen (1975); for rate-independency, it must be positively homogeneous of degree-one with respect to the flux  $\dot{d}$ :

$$\varphi(\dot{d}) = Y_c(d) \dot{d} + \sqcup_{\mathbb{R}^+}(\dot{d}) \quad (3)$$

In the above relationship  $Y_c(d)$  is a positive convex function of the current damage state  $d$ , here considered as a parameter, and  $\sqcup_{\mathbb{R}^+}$  is the convex indicator of non-negative reals that enforces irreversibility:

$$\sqcup_{\mathbb{R}^+}(d^*) = \begin{cases} 0 & \text{if } d^* \geq 0 \\ +\infty & \text{otherwise} \end{cases} \quad (4)$$

Likewise, damage is a constrained variable since it has to comply with the physical bounds:

$$0 \leq d \leq 1 \quad (5)$$

This can be accounted for in the present formulation either via an indicator function of the admissibility domain or using a smoothed version of it, say  $g_1(d)$ , with the relevant Karush-Kuhn-Tucker conditions

$$g_1(d) \leq 0; \quad \gamma_1 \geq 0; \quad \gamma_1 g_1(d) = 0 \quad (6)$$

It is well known that the local constitutive equations emanating from the above potentials will produce non-objective numerical solutions with respect to finite element meshes; actually, owing to strain softening, strains and damage do localise into narrow regions with high gradients and mechanical dissipation is strongly affected by mesh refinements. Objectivity can be restored by appealing to a nonlocal formulation, i.e. introducing spatial interactions into the constitutive equations to provide a suitable localization limiter Bažant and Planas (1998). To this end, in the graded damage model an explicit nonlocal constraint acting on the damage gradient is prescribed via the following Valoroso and Stolz (2022):

$$g_2(d) = \|\nabla d\| - f(d) \quad (7)$$

where the bounding function  $f(d) > 0$  may be arbitrarily nonlinear provided that it is concave; in addition, the following complementarity conditions apply:

$$g_2(d) \leq 0; \quad \gamma_2 \geq 0; \quad \gamma_2 g_2(d) = 0 \quad (8)$$

that characterize the gradient constraint (7) as non-dissipative.

As a direct consequence of nonlocality, the thermodynamic potentials are functionals of the state variables  $u$  and  $d$ , here understood as fields Germain et al. (1983). In particular, the internal energy of the rod is the Lagrangian:

$$\mathcal{E}(\varepsilon, d, \gamma_i) = \int_{\Omega} \psi(\varepsilon, d) dx + \int_{\Omega} [\gamma_1 g_1(d) + \gamma_2 g_2(d)] dx \quad (9)$$

where  $\psi$  is the local stored energy function defined by equation (1); likewise, a global pseudo-potential of dissipation is obtained by integrating the dissipation function (3) over the physical domain  $\Omega$ :

$$\mathcal{D}(\dot{d}) = \int_{\Omega} \varphi(\dot{d}) dx \quad (10)$$

The forces work-conjugate to the axial strain and damage are the Cauchy stress and the energy release rate. In particular, the former is obtained along with the equilibrium equation by zeroing the first variation of the potential energy (9) with respect to the displacement  $u$  as

$$\sigma = \omega(d) E \frac{du}{dx} \quad (11)$$

For the ensuing developments the gradient constraint is taken as:

$$g_2(d) = \left| \frac{dd}{dx} \right| - \frac{1}{l_c} \leq 0 \quad (12)$$

whence results a piece-wise linear distribution of damage along the rod. The energy release rate is a variational derivative and includes a nonlocal term originating from (12) plus two boundary conditions Miehe et al. (2010b). In particular, the first variation of the functional (9) with respect to damage followed by integration by parts yields:

$$\frac{\partial \mathcal{E}}{\partial d} \delta d^* = \left[ - \int_{\Omega} G \, dx + \left[ \left[ \gamma_2 \operatorname{sign} \left( \frac{dd}{dx} \right) \right] \right]_S + \left[ \gamma_2 \operatorname{sign} \left( \frac{dd}{dx} \right) \right]_{\partial \Omega} \right] \delta d^* \quad (13)$$

where the domain term  $G$  reads:

$$G = - \frac{\partial \psi}{\partial d} - \gamma_1 \frac{dg_1}{dd} + \frac{d}{dx} \left( \gamma_2 \operatorname{sign} \left( \frac{dd}{dx} \right) \right) \quad (14)$$

$S$  being the set of possible discontinuity points for the damage gradient. For non-dissipative internal discontinuities the (internal) jump relationships give:

$$\gamma_2^+ = \gamma_2^- = 0 \quad (15)$$

whereas the (external) natural boundary conditions read:

$$\gamma_2(x) = 0; \quad x \in \partial \Omega \quad (16)$$

which allow for non-zero damage derivatives on the outer boundary.

Damage evolution is governed by the normality rule:

$$G - Y_c(d) \leq 0, \quad \dot{d} \geq 0, \quad (G - Y_c(d)) \dot{d} = 0 \quad (17)$$

that follows from the Biot-like subdifferential inclusion:

$$- \frac{\partial \mathcal{E}}{\partial d} \in \partial \mathcal{D}(\dot{d}) \quad (18)$$

During initial loading the displacement  $u^*$  increases up to the elastic limit:

$$u_{el} = \sqrt{\frac{2 Y_c(0)}{-\omega'(0) E}} L \quad (19)$$

and the unique response is the homogeneous elastic one:

$$u^* = \frac{\sigma L}{E} \quad (20)$$

Once damage has started to grow and its spatial distribution  $d(x)$  is known, the relationship between the constant stress and the prescribed displacement can be made explicit as:

$$u^* = \frac{\sigma}{2 E} \int_{\Omega} \omega^{-1}(d(x)) \, dx \quad (21)$$

Solutions beyond the elastic limit are associated with the initiation and growth of defects and can be either homogeneous or localized; in both cases one can use a parametrization in terms of the maximum damage level  $d_m \leq 1$ .

For the homogeneous inelastic case, damage evolution requires the local strain energy to increase everywhere in the bar; this can be expressed as

$$\left( \frac{Y_c(d)}{-\omega'(d)} \right)' > 0 \quad (22)$$

where use is made of the local limit condition emanating from (17) and the prime denote differentiation with respect to the driving variable  $d$ . The above inequality is equivalent to:

$$Y_c(d) \omega''(d) - Y_c'(d) \omega'(d) > 0 \quad (23)$$

that is a necessary requirement for local stability. Condition (23) is suggested in Lorentz and Godard (2011) along with an additional strain softening condition, whereby the complementary elastic energy should decrease with damage, that is:

$$\left( \frac{\omega^2(d) Y_c(d)}{-\omega'(d)} \right)' < 0 \quad (24)$$

whereby one has

$$[Y_c'(d) \omega^2(d) + Y_c(d) 2 \omega(d) \omega'(d)] \omega'(d) - Y_c(d) \omega^2(d) \omega''(d) > 0 \quad (25)$$

Without loss of generality, for non-homogeneous damage we assume that strain localization associated with one single defect initiates at point  $x = 0$  immediately after the initial elastic limit (19) has been attained; the study can therefore be limited to half of the bar on account of the symmetry of (12).

The complementarity conditions (8) imply that the multiplier  $\gamma_2$  can be non-zero only where the nonlocal constraint (12) is met with the equality. In this case the damage field reads:

$$d(x) = d(0) - \frac{x}{l_c} \quad (26)$$

and the constraint set coincides with the interval  $[0, l_m]$ , being

$$l_m = l_c d(0) = l_c d_m \leq l_c \quad (27)$$

the half-width of the localization band, see also Figure 2.

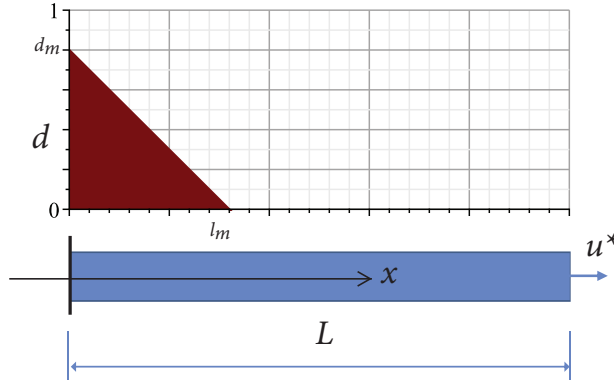


Figure 2: One-dimensional rod. Damage distribution for localized solution.

For damage evolution ( $\dot{d} > 0$ ) one has from (17) the differential problem:

$$Y(d(x)) - \frac{d\gamma_2}{dx} = Y_c(d(x)) \quad (28)$$

where the local damage-driving force reads:

$$Y = -\frac{\partial \psi}{\partial d} = \frac{-\omega'(d) \sigma^2}{\omega^2(d) 2E} \quad (29)$$

Relationship (28) is a first-order differential equation subject to two boundary conditions; the first one allows to compute the (uniform) stress  $\sigma$  as a function of the driving variable  $d_m$  and the second one is needed to set the integration constant for the Lagrange multiplier field  $\gamma_2$ . The latter is certainly nihil either on the boundary of the active constraint set defined by  $g_2(d) = 0$ , either where the gradient of damage is discontinuous, or on the outer boundary of the domain, where condition (16) holds. Therefore, integration of (28) between 0 and  $l_m$ , which correspond to two discontinuity points for the damage gradient, provides the *averaged limit condition* Valoroso and Stolz (2022):

$$\int_0^{l_m} Y(d(x)) dx = \int_0^{l_m} Y_c(d(x)) dx \quad (30)$$

The integrals are computed via  $u$ -substitution in the form

$$\int_0^{l_m} y(d(x)) dx = -l_c \int_{d(0)}^{d(l_m)} y(d) dd \quad (31)$$

and one obtains the stress as a function of the maximum damage level  $d_m$  as:

$$\sigma(d_m) = \left[ \frac{2E}{\omega^{-1}(d_m) - 1} H(d_m) \right]^{\frac{1}{2}} \quad (32)$$

where  $H(d_m)$  is the definite integral:

$$H(d_m) = \int_0^{d_m} Y_c(d) dd \quad (33)$$

and the integrand  $Y_c(d)$  is the constitutive function, which can in turn be determined in a way consistent with a cohesive model. To this end re-write equation (21) for half of the bar and split the integral into two parts, respectively accounting for damage behaviour and a purely elastic response:

$$u^* = \frac{\sigma}{E} \left[ \int_0^{l_m} [\omega^{-1}(d(x)) - 1] dx + L \right] = \frac{1}{2} w + \frac{\sigma L}{E} \quad (34)$$

In the above equation  $w$  is the apparent opening displacement across the localization band; it can be expressed in terms of the chosen parametrization as:

$$w(d_m) = \frac{2\sigma(d_m)}{E} l_c F(d_m) \quad (35)$$

where the non-dimensional term  $F(d_m)$  reads:

$$F(d_m) = \int_0^{d_m} (\omega^{-1}(d) - 1) dd \quad (36)$$

and depends only upon the assumed form of the degradation function  $\omega(d)$ .

Relationships (32) and (35) are used to determine the constitutive function  $Y_c(d)$  by requiring that the macroscopic response of the damageable rod be equivalent to that of an elastic bar in which the localization band is replaced by a cohesive interface of given properties. In particular, we consider the linear softening law depicted in Figure 3, whose analytical expression reads:

$$\sigma = \sigma_c \left( 1 - \frac{\sigma_c}{2G_c} w \right) \quad (37)$$

where  $\sigma_c$  and  $G_c$  respectively denote the peak stress and the fracture energy.

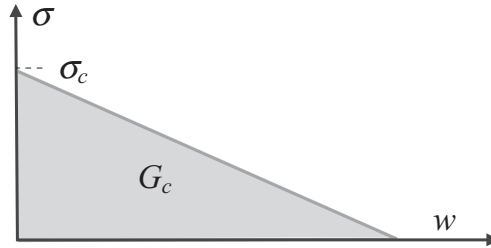


Figure 3: Linear softening function.

Substitution of (35) into (37) and solution for  $\sigma(d_m)$  provides the stress as a function of the maximum damage  $d_m$  as:

$$\sigma(d_m) = \frac{\sigma_c}{1 + \lambda F(d_m)} \quad (38)$$

where  $\lambda$  is the non-dimensional parameter:

$$\lambda = \frac{l_c}{l_{coh}} \quad (39)$$

expressing the ratio between the characteristic length  $l_c$  of the graded damage model and the length scale  $l_{coh}$  of the cohesive zone Hillerborg et al. (1976):

$$l_{coh} = \frac{E G_c}{\sigma_c^2} \quad (40)$$

For a given  $d_m$ , the value  $H(d_m)$  of the integral (33) follows from substitution of (38) into (32) as:

$$H(d_m) = \frac{\omega^{-1}(d_m) - 1}{2E} \left( \frac{\sigma_c}{1 + \lambda F(d_m)} \right)^2 \quad (41)$$

Motivated by stability arguments that are being illustrated later on, we choose for the degradation function the quadratic expression:

$$\omega = (1 - d)^2 \quad (42)$$

whereby one has from (36):

$$F(d_m) = \frac{d_m^2}{1 - d_m} \quad (43)$$

while (32) provides the following expression for the (uniform) stress:

$$\sigma(d_m) = \sigma_c \frac{1 - d_m}{\lambda d_m^2 + 1 - d_m} \quad (44)$$

with the limits

$$\lim_{d_m \rightarrow 0} \sigma(d_m) = \sigma_c; \quad \lim_{d_m \rightarrow 1} \sigma(d_m) = 0 \quad (45)$$

The constitutive function  $Y_c(d)$  is computed by differentiation of (41) as:

$$Y_c(d) = \frac{\sigma_c^2}{E} \frac{1 + \lambda d^2(d - 3)}{(\lambda d^2 + 1 - d)^3} \quad (46)$$

and the relevant limits read:

$$Y_c(0) = \lim_{d \rightarrow 0} Y_c(d) = \frac{\sigma_c^2}{E}; \quad \lim_{d \rightarrow 1} Y_c(d) = \frac{\sigma_c^2}{E} \frac{1 - 2\lambda}{\lambda^3} \quad (47)$$

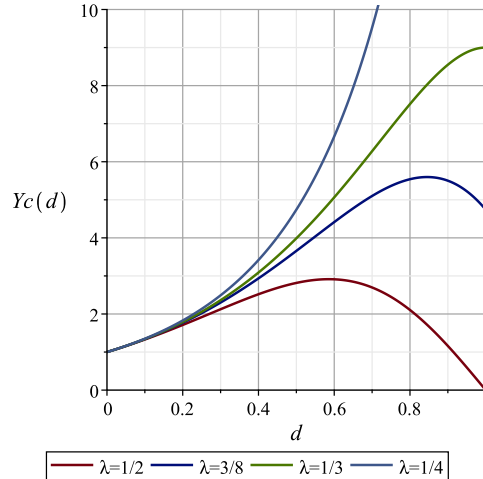


Figure 4: The constitutive function  $Y_c$  consistent with linear softening.

Figure 4 depicts the function  $Y_c(d)$  normalized to  $Y_c(0)$  for different values of the parameter  $\lambda$ , which determines the properties of the function  $Y_c(d)$  itself. In practice, a *safe value* of  $\lambda$  to be used in numerical computations Valoroso and Stolz (2022) can be taken in a way to comply with conditions (23) and (25).

For the case at hand the local stability requirement (23) provides:

$$\lambda < \frac{(d-2)\sqrt{d^4 - 4d^3 + 40d^2 - 72d + 36} + d^3 - 4d^2 - 10d + 12}{8d^4 - 36d^3 + 24d^2} \quad (48)$$

with limit

$$\lim_{d \rightarrow 1} \lambda = \frac{1}{2} \quad (49)$$

On the other hand, the strain softening condition (25) implies:

$$0 < \lambda < \frac{1 + (1-d)^2}{2d} \quad (50)$$

The above relationships define the admissible region for  $\lambda$  that is shaded in Figure 5. Clearly, any positive value of  $\lambda$  lower than 0.5 allows to fulfill both conditions for each  $d \in [0, 1]$ .

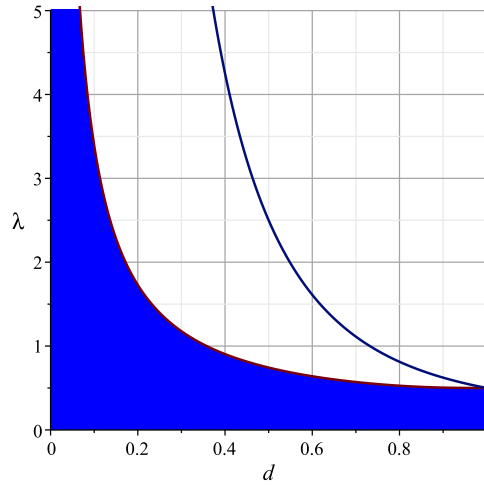


Figure 5: Admissible region for parameter  $\lambda$ .

For a given damage distribution the relationship between the stress and the displacement  $u^*$  is obtained from equation (21) as:

$$\sigma(d_m) = \frac{E u^*}{L} \frac{1 - d_m}{(\beta d_m^2 + 1 - d_m)} \quad (51)$$

with

$$\beta = \frac{l_c}{L} \quad (52)$$

Evidently, in the present context knowledge of the damage distribution is equivalent to knowledge of the constraint set  $[0, l_m]$ , where the integral in equation (21) is non-trivial and the Lagrange multiplier  $\gamma_2$  is non-zero.

Evaluation of the multiplier  $\gamma_2$  amounts to compute the integral of the differential equation (28). To this end use is made of the chain rule as:

$$\frac{d\gamma_2}{dx} = \gamma_2'(d) \frac{dd}{dx} = -\frac{1}{l_c} \gamma_2'(d) \quad (53)$$

to get the integral as:

$$\frac{1}{l_c} \gamma_2(d) = \frac{-\sigma^2(d_m)}{2E\omega(d)} + \frac{\sigma_c^2}{E} \frac{d(2-d)}{2(\lambda d^2 + 1 - d)^2} + C \quad (54)$$

The integration constant  $C$  is obtained using one of the two boundary conditions on  $\gamma_2$ , i.e.  $\gamma_2(0) = \gamma_2(d_m) = 0$ , that is:

$$C = \frac{\sigma^2(d_m)}{2E} \quad (55)$$

whereby one has:

$$\begin{aligned}\gamma_2(d) &= \frac{-\sigma^2(d_m) l_c}{2E} (\omega^{-1}(d) - 1) + \frac{\sigma_c^2 l_c}{E} \frac{d(2-d)}{2(\lambda d^2 + 1 - d)^2} \\ &= \frac{l_c}{2E} \frac{d(2-d)}{(1-d)^2} [\sigma^2(d) - \sigma^2(d_m)]\end{aligned}\quad (56)$$

Equation (56) describes the variation of the multiplier  $\gamma_2$  within the active constraint interval and depends upon  $d_m$ , which is a fixed value, and  $d = d(x)$ , which is a function of the abscissa  $x$  along the bar. It is immediately recognized that the Lagrange multiplier  $\gamma_2$  is zero either at  $x = 0$ , where  $d = d_m$ , and at  $x = l_m$ , where  $d = 0$ . Moreover, its maximum value within the interval occurs at point  $\bar{x}$  where  $Y(x) = Y_c(d(x))$  owing to the differential relationship (28).

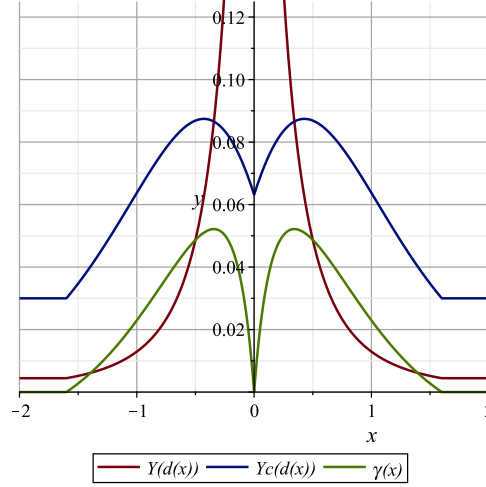


Figure 6: One-dimensional rod. A typical spatial distribution of  $Y$ ,  $Y_c$  and  $\gamma_2$  corresponding to the symmetric localized solution with a single defect.

A typical spatial distribution of the Lagrange multiplier  $\gamma_2(x)$  within the symmetric localization band is depicted in Figure 6 along with the local damage-driving force  $Y$  and the constitutive function  $Y_c$ .

The response of the elasto-damaging bar is clearly dependent upon the length scales  $l_c$  and  $l_{coh}$  via the non-dimensional parameter  $\lambda$  defined by (39) and from the geometric factor  $\beta$  given by (52).

Actually, by comparison of equation (44) with (51) one has:

$$u^*(d_m) = \frac{\sigma_c L}{E} \frac{\beta d_m^2 + 1 - d_m}{\lambda d_m^2 + 1 - d_m} \quad (57)$$

This relationship allows to obtain the condition under which the response of the rod is stable under displacement control, i.e. it does not exhibit a snap-back. This requires the end-displacement  $u^*$  to be an increasing function of the maximum damage level  $d_m$ , that is:

$$\frac{\partial u^*}{\partial d_m} = \frac{\sigma_c L}{E} \frac{(\beta - \lambda)(2d_m - d_m^2)}{\lambda d_m^2 + 1 - d_m} > 0 \quad (58)$$

whereby one obtains the condition that governs the stability of the response for the damaging tensile bar under displacement control

$$\beta > \lambda \Leftrightarrow L < l_{coh} \quad (59)$$

The stability condition strongly depends upon the expressions of the degradation function (42) and of the constitutive function (46). Actually, taking for  $Y_c$  the constant function, i.e.  $Y_c(0)$  given by (47), and the quadratic degradation function (42) one obtains:

$$\sigma(d_m) = \frac{2\sigma_c(1-d_m)}{\sqrt{4-2d_m}} \quad (60)$$

in place of (44) and

$$u^*(d_m) = \frac{\sigma_c L}{E} \frac{2(\beta d_m^2 + 1 - d_m)}{\sqrt{4 - 2d_m}} \quad (61)$$

that replaces (57). The stability condition now reads:

$$\beta > \frac{3 - d_m}{d_m (8 - 3d_m)} \quad (62)$$

whereby one infers that there is always a snap back right after the elastic limit no matter how short is the bar since the right-hand side of (62) diverges for  $d_m \rightarrow 0$ . This can slow down convergence in the solution of a Finite Element problem and should be avoided as much as possible.

However, there exist situations that are even more harmful. In this respect, consider the case of a linear degradation function

$$\bar{\omega}(d) = 1 - d \quad (63)$$

and a constant elastic limit

$$\bar{Y}_c = \frac{\sigma_c^2}{2E} \quad (64)$$

In this case one obtains the stress and the end displacement as:

$$\sigma(d_m) = \sigma_c \sqrt{1 - d_m} \quad (65)$$

$$u^*(d_m) = \frac{\sigma_c L}{E} (1 - \beta d_m - \beta \ln(1 - d_m)) \quad (66)$$

The stability condition now reads:

$$\beta > \frac{1}{\ln(1 - d_m) + 3d_m} \quad (67)$$

Clearly, the right-hand side of (67) diverges for both  $d_m \rightarrow 0$  and for  $d_m \rightarrow 1 - \exp(-3d_m) \simeq 0.94048$ .

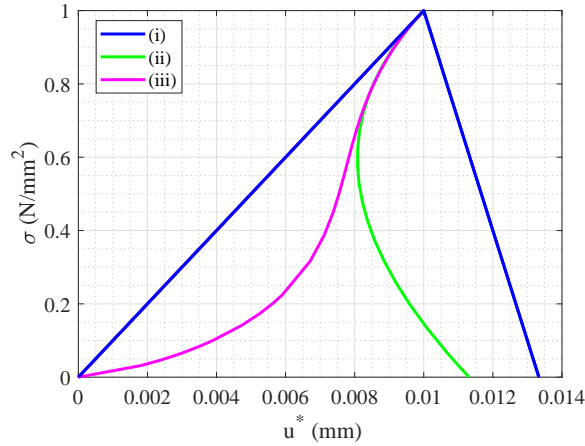


Figure 7: One dimensional rod. Normalized stress-displacement responses obtained for different choices of the constitutive functions  $\omega(d)$  and  $Y_c(d)$ .

Figure 7 depicts the  $\sigma - u^*$  response of the bar for the different choices of the constitutive functions  $\omega(d)$  and  $Y_c(d)$  considered above, that is:

- (i) quadratic degradation and non-constant limit  $Y_c(d)$  that realizes the equivalence with linear softening;
- (ii) quadratic degradation and constant limit  $Y_c = \sigma_c^2/E$ ;
- (iii) linear degradation and constant limit  $Y_c = \sigma_c^2/2E$ .

For all these cases the non-dimensional parameters respectively defined by (39) and (52) are such that  $\lambda \leq 0.5$  and  $\beta > \lambda$ , which correspond to a rod that can be considered a short one.

### 3 The block with cohesive interface

Generally speaking, a cohesive law is a relationship between a displacement discontinuity vector, which is understood as the interface strain, and a surface traction vector playing the role of the stress. For the developments that follow attention will be restricted to mode-I opening; tractions and displacement jumps will then be normal to the interface while negative relative displacements will be left out for notational simplicity.

As a model problem consider the structure in Figure 8, consisting of a rigid block connected to a fixed support via a damageable adhesive layer of negligible thickness Volokh (2004). A monotonic increase of the end-displacement  $\delta$  produces a uniform rotation of the block but a non-uniform distribution of damage, which starts nucleating from the left edge with non-zero gradient.

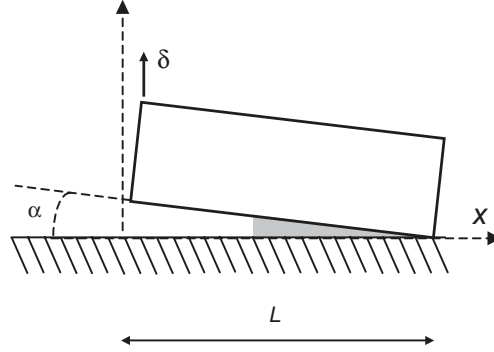


Figure 8: The rigid-block problem.

Denoting by  $w$  the opening displacement across the interface, a stored energy function from which one can obtain a (local) cohesive law using a damage-based formulation reads Valoroso and Champaney (2006):

$$\tilde{\psi}(w, d) = \frac{1}{2} \omega(d) k w^2 \quad (68)$$

where  $k$  is the (undamaged) interface stiffness in tension.

For the problem at hand the kinematics of deformation is completely described by a single parameter, i.e. the rotation  $\alpha$ , here assumed to be small in the usual sense. Therefore, one has the opening displacement:

$$w(x) = \alpha (L - x) \quad (69)$$

while the stress-like variables read:

$$t(x, d) = \frac{\partial \tilde{\psi}(w, d)}{\partial w} = \omega(d) k \alpha (L - x) \quad (70)$$

$$\tilde{Y}(x, d) = -\frac{\partial \tilde{\psi}(w, d)}{\partial d} = -\omega'(d) \frac{1}{2} k \alpha^2 (L - x)^2$$

The governing equations of a nonlocal interface model based on the graded damage concept are formally identical to those developed in Section 2 for the tensile rod with two minor modifications. In particular, the stored energy function (1) has to be replaced by (68), while the function  $\tilde{Y}_c(d)$  is now directly prescribed, e.g. based on the shape of a chosen traction-separation relationship.

For instance, a constitutive function  $\tilde{Y}_c(d)$  that yields the (local) bilinear cohesive law of Figure 9 reads:

$$\tilde{Y}_c(d) = \frac{-\omega'(d) G_0 G_c^2}{[G_0 + (G_c - G_0) \omega(d)]^2} \quad (71)$$

to which corresponds the work of separation:

$$\int_0^{+\infty} \tilde{Y}_c(d) \dot{d} dt = - \int_0^1 \tilde{Y}_c(\omega) d\omega = G_c \quad (72)$$

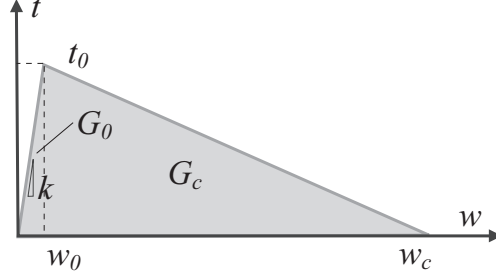


Figure 9: Bilinear cohesive law

where  $G_0$  and  $G_c$  respectively denote the initial energy threshold and the interface fracture toughness:

$$G_0 = \frac{1}{2}k w_0^2; \quad G_c = \frac{1}{2}k w_0 w_c \quad (73)$$

Without loss of generality, in the remainder we shall assume equations (12) and (42) to hold; moreover, the length scale  $l_c$  of the nonlocal interface model is supposed to be greater than the width  $L$  of the block.

The equilibrium path of the structure can be traced using the balance of moments about the center of rotation:

$$P L = \int_{\Omega} t(x, d) (L - x) dx \quad (74)$$

$\Omega$  being the physical domain  $[0, L]$  and  $P$  the reaction force corresponding to the prescribed displacement  $\delta$ . During initial loading the latter increases up to the elastic limit  $\delta_0$  given by:

$$\delta_0 = \sqrt{\frac{2G_0}{k}} = \alpha_0 L \quad (75)$$

that is first attained when the local limit condition  $\tilde{Y} = \tilde{Y}_c(0)$  is met. This state corresponds to damage nucleation at  $x = 0$  and from this point onwards loading can be effectively parametrized in terms of the size  $l_m > 0$  of the damaged portion of the domain of interest.

For  $l_m \leq l_c$  the length  $l_m$  does also coincide with the size of the active constraint set (i.e. where  $g_2(d) = 0$ ) and the adopted parametrization is fully equivalent to the one given in terms of the maximum damage  $d_m$  defined as:

$$d_m = \min \left\{ 1, \frac{l_m}{l_c} \right\} \quad (76)$$

It is worth emphasizing that, unlike the case of the tensile rod with a single evolving defect, for the problem at hand the constraint set translates along the interface once the damage process zone has fully developed. In particular, this occurs when the size of the damaged region  $l_m$  equals the length scale  $l_c$ ; to account for this case, the (piece-wise) linear damage function that is prescribed via the gradient constraint (12) is conveniently defined as:

$$d(x) = \max \left\{ 0, d_m - \frac{x - c}{l_c} \right\} \quad (77)$$

where the (finite) size of the fully damaged subdomain reads:

$$c = \max \left\{ 0, l_m - l_c \right\} \quad (78)$$

As discussed in Section 2, owing to gradient-dependence the normality rule yields the differential equation (28); the latter now admits two sets of boundary conditions for the opening angle  $\alpha$  and the Lagrange multiplier  $\gamma_2$ .

For the rigid block problem the averaged limit condition reads:

$$\int_0^H \tilde{Y}(x, d(x)) dx = \int_0^H \tilde{Y}_c(d(x)) dx \quad (79)$$

Table 1: Data set for the rigid block problem

$L = 2 \text{ mm};$	$k = 800 \text{ N/mm}^3$
$G_c = 0.25 \text{ N/mm};$	$G_0 = 0.025 \text{ N/mm}$

where  $H$  denotes the size of the active process zone portion that is contained within the physical domain  $[0, L]$ :

$$H = \min \left\{ l_m, L \right\} \quad (80)$$

With this notation in hand, balance of moments about the center of rotation can be expressed as:

$$P L = \int_c^H \omega(d) k \hat{\alpha} (L - x)^2 dx + \int_H^L k \hat{\alpha} (L - x)^2 dx \quad (81)$$

whereby one obtains the different branches of the equilibrium path by distinguishing the different possible cases for the integration limits of equation (79), which in turn take into account the boundary conditions (16) for the Lagrange multiplier field and the internal jump conditions (15), if any.

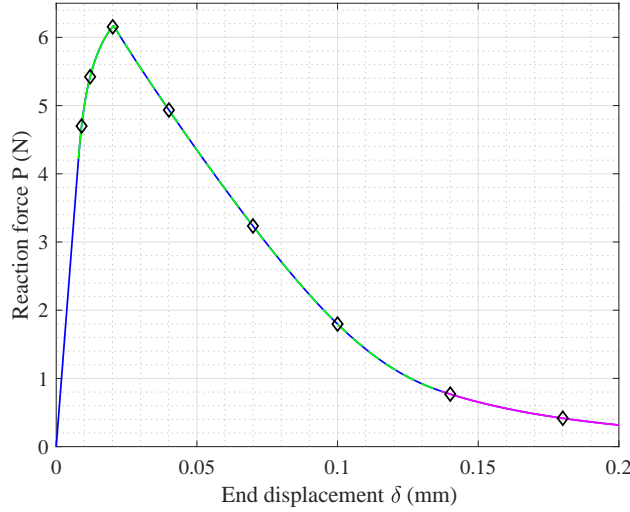


Figure 10: Equilibrium curve for the rigid-block problem.

**Phase 1. Linear elastic** The initial linear elastic phase is purely local; the limit value for the displacement is given by (75), to which corresponds the reaction force:

$$P_0 = \sqrt{2 G_0 k} \frac{L}{3} \quad (82)$$

**Phase 2. Damage nucleation and growth for  $0 < l_m \leq L$**  In this case use of the integral limit condition (79) allows to compute the opening angle  $\alpha$  as a function of the length  $l_m$  (driving variable) as:

$$\hat{\alpha}_1 = \alpha_0 \sqrt{\frac{G_c l_c^2 L^2 (2 l_c - l_m)}{A_1 A_2}} \quad (83)$$

with

$$A_1 = \left[ \frac{l_m^3}{6} - \frac{2}{3} (l_c + L) l_m^2 + (L + 2 l_c) L l_m - 2 L^2 l_c \right] \quad (84)$$

$$A_2 = [(G_0 - G_c)(l_m^2 - 2 l_c l_m) - G_c l_c^2] \quad (85)$$

and limits

$$\hat{\alpha}_1^0 = \lim_{l_m \rightarrow 0} \hat{\alpha}_1 = \alpha_0 \quad (86)$$

$$\hat{\alpha}_1^L = \lim_{l_m \rightarrow L} \hat{\alpha}_1 = \alpha_0 \sqrt{\frac{6 G_c l_c^2 (2 l_c - L)}{(4 l_c - 3 L) [(l_c - L)^2 G_c - (L - 2 l_c) G_0 L]}} \quad (87)$$

Obviously, the limit (86) coincides with the opening angle  $\alpha_0$  defined by (75) whereas the upper limit (87) marks the end of the domain of validity of relationship (83), to which corresponds by equilibrium the end reaction force:

$$\hat{P}_1 = \left[ L^3 l_c^2 + (l_m - 3 l_c) l_m^2 L^2 - \frac{(l_m - 4 l_c) l_m^3 L}{2} + \frac{(l_m - 5 l_c) l_m^4}{10} \right] \frac{k \hat{\alpha}_1}{3 l_c^2 L} \quad (88)$$

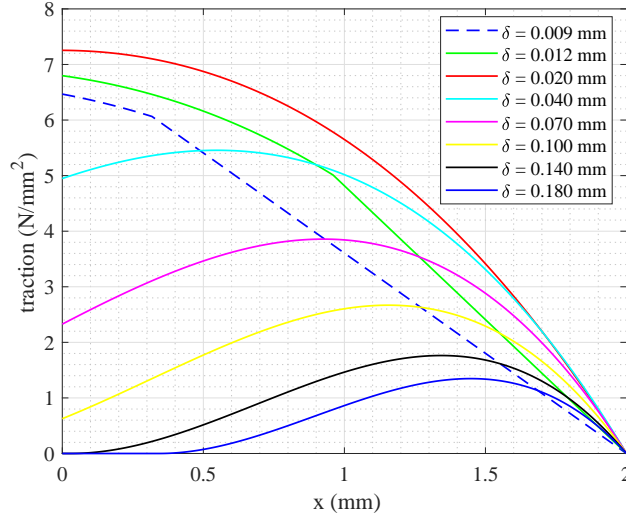


Figure 11: Tractions distributions along the interface at varying end-displacement  $\delta$ .

**Phase 3. Damage growth for  $L \leq l_m \leq l_c$**  When the driving variable  $l_m$  grows beyond the length  $L$ , the zero-damage boundary would be located outside the physical domain of the interface. In this case the boundary conditions for the Lagrange multiplier and the limit condition (79) yield an averaged equality over the entire domain  $[0, L]$ , whereby one obtains another nonlinear branch of the equilibrium path defined by the following:

$$\hat{\alpha}_2 = \alpha_0 \sqrt{\frac{6 G_c^2 l_c^4 (L + 2 l_c - 2 l_m)}{B_1 B_2 B_3}} \quad (89)$$

with

$$B_1 = L + 4 l_c - 4 l_m \quad (90)$$

$$B_2 = (l_c - l_m)^2 G_c - l_m (l_m - 2 l_c) G_0 \quad (91)$$

$$B_3 = (L - l_m + l_c)^2 G_c - (L - l_m)(L - l_m + 2 l_c) G_0 \quad (92)$$

The corresponding value of the reaction force reads:

$$\hat{P}_2 = \frac{k L^2}{30 l_c^2} [10 l_c^2 + (5 L - 20 l_m) l_c + L^2 - 5 L l_m + 10 l_m^2] \hat{\alpha}_2 \quad (93)$$

**Phase 4. Crack propagation** For  $l_m > l_c$  there exists a fully damaged region of finite size  $c$  defined by (78); the latter can be taken as the driving variable for computing the last part of the equilibrium curve because in this case the non-trivial limit condition reduces to an averaged equality over the interval  $[c, L]$  on account of the jump relationships (15).

The opening angle is now computed as:

$$\hat{\alpha}_3 = \frac{\alpha_0}{(L - c)^2} \sqrt{\frac{6 G_c^2 l_c^2 L^2}{G_0 [G_c (L - c)^2 - G_0 (-L + c - l_c)(-L + c + l_c)]}} \quad (94)$$

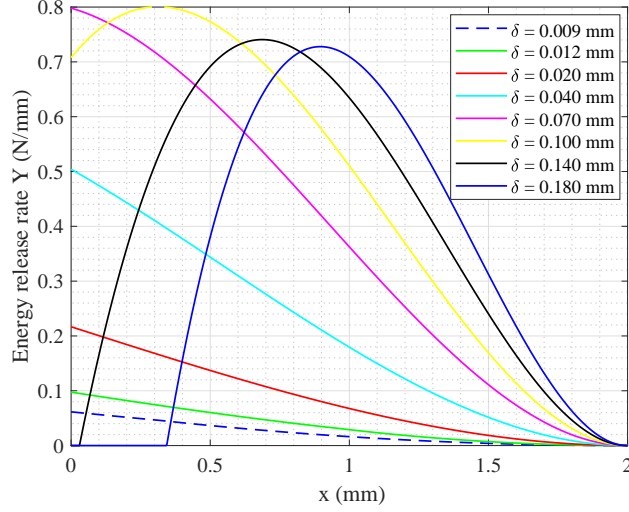


Figure 12: Damage-conjugate force  $\tilde{Y}$  along the interface at varying end-displacement  $\delta$ .

whereas the equilibrium equation yields:

$$\hat{P}_3 = \frac{k (L - c)^5}{30 l_c^2 L} \hat{\alpha}_3 \quad (95)$$

As expected, the reaction force (95) converges to zero when the portion of the active damage process zone lying within the physical domain progressively shrinks and collapses to a point.

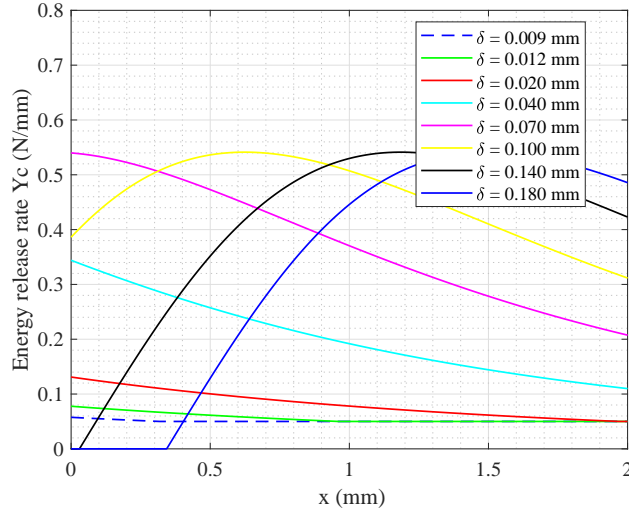


Figure 13: Threshold function  $\tilde{Y}_c$  along the interface at varying end-displacement  $\delta$ .

The complete equilibrium path for the block delamination problem is depicted in Figure 10. The curve corresponds to a length scale  $l_c = 6 \text{ mm}$  and to the data set of Table 1. The different colors on the plot are used to distinguish the four branches of the theoretical solution whereas the points highlighted on the load-deflection curve indicate the stations selected for the plots of Figure 11, which shows the distribution of the surface tractions along the interface for different damage levels.

Unlike the case of a local model, where the profile of the surface tractions would replicate the bilinear shape of the traction-separation curve consequent to (71), due to gradient-dependence the tractions distribution in the present case changes continuously from a bilinear shape to an exponential-like one for increasing end-displacement  $\delta$ .

Moreover, it is noted that the differential character of the constitutive relationship allows for point-wise values of the surface tractions higher than the peak stress  $\sqrt{2k}G_0$  of the underlying local model. Likewise, the point-wise values of the damage-conjugate variable  $\tilde{Y}$  can exceed those of the limit function  $\tilde{Y}_c$  owing to the averaged character of the limit condition. This behaviour is clearly put forward in Figures 12 and 13, that have been plotted using the same scale to ease the comparison.

It is also worth noting that functions  $\tilde{Y}$  and  $\tilde{Y}_c$  do share only one common point-wise value over the physical domain  $[0, L]$ . This corresponds to the extremum point, which is indeed a maximum because of the obvious sign constraint, of the Lagrange multiplier field  $\gamma_2$  that is used to enforce the nonlocal, gradient constraint, see e.g. Figure 14.

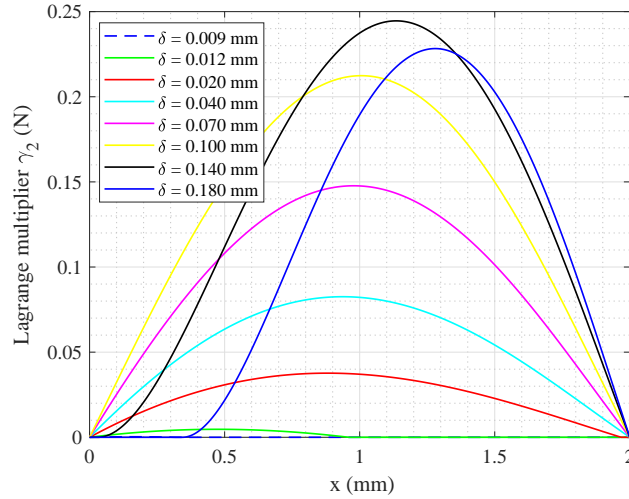


Figure 14: Lagrange multiplier  $\gamma_2$  along the interface at varying end-displacement  $\delta$ .

## 4 Closure

Based on the graded damage formulation contributed in Valoroso and Stolz (2022) two problems in one dimension have been discussed and the relevant analytical solutions computed to be used as a reference for finite element procedures. In the tensile rod problem the uniform stress is obtained from the averaged limit condition and the constitutive function  $Y_c$  is determined in a way to produce a global response curve that is consistent with a cohesive zone model with linear softening. On the other hand, in the block delamination problem the constitutive function  $Y_c$  is prescribed based on a local cohesive model while the integral limit condition provides the parameter governing the kinematics of deformation. In this case one obtains a global equilibrium curve that depends from the length scale since the effect of gradient-dependence is that of relaxing the surface tractions in that they are no longer constrained to the shape of the underlying local softening curve.

## References

- Z.P. Bažant and J. Planas. *Fracture and Size Effect in Concrete and Other Quasibrittle Materials*. CRC Press, London, 1998. doi:<https://doi.org/10.1201/9780203756799>.
- D. François, A. Pineau, and A. Zaoui. *Mechanical Behaviour of Materials. Volume II: Fracture Mechanics and Damage*. Solid Mechanics and Its Applications. Springer, 2013. ISBN 978-94-007-4929-0. doi:[10.1007/978-94-007-4930-6](https://doi.org/10.1007/978-94-007-4930-6).
- F. Armero and K. Garikipati. An analysis of strong discontinuities in multiplicative finite strain plasticity and their relation with the numerical simulation of strain localization in solids. *International Journal of Solids and Structures*, 33(20):2863–2885, 1996. ISSN 0020-7683. doi:[10.1016/0020-7683\(95\)00257-X](https://doi.org/10.1016/0020-7683(95)00257-X).
- N. Mões, J. Dolbow, and T. Belytschko. A finite element method for crack growth without remeshing. *International Journal for Numerical Methods in Engineering*, 46(1):131–150, 1999. doi:[10.1002/\(SICI\)1097-0207\(19990910\)46:1<131::AID-NME726>3.0.CO;2-J](https://doi.org/10.1002/(SICI)1097-0207(19990910)46:1<131::AID-NME726>3.0.CO;2-J).

- N. Moës, C. Stolz, P.-E. Bernard, and N. Chevaugeon. A level set based model for damage growth: The thick level set approach. *International Journal for Numerical Methods in Engineering*, 86(3):358–380, 2011. ISSN 1097-0207. doi:10.1002/nme.3069.
- G.I. Barenblatt. The mathematical theory of equilibrium cracks in brittle fracture. In H.L. Dryden, Th. von Kármán, G. Kuerti, F.H. van den Dungen, and L. Howarth, editors, *Advances in Applied Mechanics*, volume 7, pages 55–129. Elsevier, 1962. doi:10.1016/S0065-2156(08)70121-2.
- G. Alfano. On the influence of the shape of the interface law on the application of cohesive-zone models. *Composites Science and Technology*, 66(6):723–730, 2006. ISSN 0266-3538. doi:10.1016/j.compscitech.2004.12.024.
- Y. Mi, M. A. Crisfield, G. A. O. Davies, and H. B. Hellweg. Progressive delamination using interface elements. *Journal of Composite Materials*, 32(14):1246–1272, 1998. doi:10.1177/002199839803201401.
- G. Pijaudier-Cabot and Z.P. Bažant. Nonlocal damage theory. *Journal of Engineering Mechanics*, 113(10):1512–1533, 1987. doi:10.1061/(ASCE)0733-9399(1987)113:10(1512).
- M.G.D. Geers, R. De Borst, W.A.M. Brekelmans, and R.H.J. Peerlings. Strain-based transient-gradient damage model for failure analyses. *Computer Methods in Applied Mechanics and Engineering*, 160(1-2):133 – 153, 1998. ISSN 0045-7825. doi:10.1016/S0045-7825(98)80011-X.
- R.H.J. Peerlings, R. De Borst, W.A.M. Brekelmans, and J.H.P. De Vree. Gradient enhanced damage for quasi-brittle materials. *International Journal for Numerical Methods in Engineering*, 39(19):3391–3403, 1996. ISSN 1097-0207. doi:10.1002/(SICI)1097-0207(19961015)39:19<3391::AID-NME7>3.0.CO;2-D.
- B. Bourdin, G.A. Francfort, and J.-J. Marigo. Numerical experiments in revisited brittle fracture. *Journal of the Mechanics and Physics of Solids*, 48(4):797 – 826, 2000. ISSN 0022-5096. doi:10.1016/S0022-5096(99)00028-9.
- C. Miehe, M. Hofacker, and F. Welschinger. A phase field model for rate-independent crack propagation: Robust algorithmic implementation based on operator splits. *Computer Methods in Applied Mechanics and Engineering*, 199(45):2765 – 2778, 2010a. ISSN 0045-7825. doi:10.1016/j.cma.2010.04.011.
- C. Miehe, F. Welschinger, and M. Hofacker. Thermodynamically consistent phase-field models of fracture: Variational principles and multi-field fe implementations. *International Journal for Numerical Methods in Engineering*, 83(10):1273–1311, 2010b. doi:10.1002/nme.2861.
- G. Alfano, L. Rosati, and N. Valoroso. A displacement-like finite element model for J2 elastoplasticity: Variational formulation and finite-step solution. *Computer Methods in Applied Mechanics and Engineering*, 155(3-4):325 – 358, 1998. ISSN 0045-7825. doi:10.1016/S0045-7825(97)00171-0.
- N. Valoroso and C. Stolz. Graded damage in quasi-brittle solids. *International Journal for Numerical Methods in Engineering*, 123(11):2467–2498, 2022. doi:10.1002/nme.6947.
- E. Lorentz and V. Godard. Gradient damage models: Toward full-scale computations. *Computer Methods in Applied Mechanics and Engineering*, 200(21-22):1927 – 1944, 2011. ISSN 0045-7825. doi:10.1016/j.cma.2010.06.025.
- J.-Y. Wu. A unified phase-field theory for the mechanics of damage and quasi-brittle failure. *Journal of the Mechanics and Physics of Solids*, 103:72 – 99, 2017. ISSN 0022-5096. doi:10.1016/j.jmps.2017.03.015.
- A. Hillerborg, M. Modéer, and P.-E. Petersson. Analysis of crack formation and crack growth in concrete by means of fracture mechanics and finite elements. *Cement and Concrete Research*, 6(6):773–781, 1976. ISSN 0008-8846. doi:10.1016/0008-8846(76)90007-7.
- M. Latifi, F.P. van der Meer, and L.J. Sluys. An interface thick level set model for simulating delamination in composites. *International Journal for Numerical Methods in Engineering*, 111(4):303–324, 2017. doi:10.1002/nme.5463.
- T.T. Nguyen, J. Yvonnet, Q.-Z. Zhu, M. Bornert, and C. Chateau. A phase-field method for computational modeling of interfacial damage interacting with crack propagation in realistic microstructures obtained by microtomography. *Computer Methods in Applied Mechanics and Engineering*, 312:567–595, 2016. ISSN 0045-7825. doi:10.1016/j.cma.2015.10.007.
- B. Halphen and Quoc Son Nguyen. Sur les matériaux standard généralisés. *Journal de Mécanique*, 14:39–63, 1975.
- P. Germain, Q.S. Nguyen, and P. Suquet. Continuum Thermodynamics. *Journal of Applied Mechanics*, 50(4b):1010–1020, 1983. doi:10.1115/1.3167184.
- K. Y. Volokh. Comparison between cohesive zone models. *Communications in Numerical Methods in Engineering*, 20(11):845–856, 2004. doi:10.1002/cnm.717.
- N. Valoroso and L. Champaney. A damage-mechanics-based approach for modelling decohesion in adhesively bonded assemblies. *Engineering Fracture Mechanics*, 73(18):2774–2801, 2006. ISSN 0013-7944. doi:10.1016/j.engfracmech.2006.04.029.